Electron−Hole Asymmetry in the Rare-Earth Manganates: A Comparative Study of the Hole- and the Electron-Doped Materials

K. Vijaya Sarathy,[†] P. V. Vanitha,[†] Ram Seshadri,[‡] A. K. Cheetham,[§] and C. N. R. Rao*[,†,‡,§]

Chemistry and Physics of Materials Unit, Jawaharlal Nehru Centre for Advanced Scientific Research, Jakkur P.O., Bangalore 560 064, India, and Solid State and Structural Chemistry Unit, Indian Institute of Science, Bangalore 560 012, India, and Materials Research Laboratory, University of California, Santa Barbara, California 93106

Received June 6, 2000. Revised Manuscript Received December 18, 2000

Properties of the hole-doped $Ln_{1-x}A_xMnO_3$ (Ln = rare earth, A = alkaline earth, $x < 0.5$) are compared with those of the electron-doped compositions ($x > 0.5$). Charge ordering is the dominant interaction in the latter class of manganates unlike ferromagnetism and metallicity in the hole-doped materials. Properties of charge-ordered (CO) compositions in the hole- and electron-doped regimes, $Pr_{0.64}Ca_{0.36}MnO_3$ and $Pr_{0.36}Ca_{0.64}MnO_3$, differ markedly. Thus, the CO state in the hole-doped $Pr_{0.64}Ca_{0.36}MnO_3$ is destroyed by magnetic fields and by substitution of Cr^{3+} or Ru^{4+} (3%) in the Mn site, while the CO state in the electron-doped $Pr_{0.36}Ca_{0.64}MnO_3$ is essentially unaffected. It is not possible to induce long-range ferromagnetism in the electron-doped manganates by increasing the Mn−O−Mn angles up to 165 and 180° as in $La_{0.33}Ca_{0.33}Sr_{0.34}MnO_3$; application of magnetic fields and Cr/Ru substitution (3%) do not result in long-range ferromagnetism and metallicity. Application of magnetic fields on the Cr/Ru-doped, electron-doped manganates also fails to induce metallicity. These unusual features of the electron-doped manganates suggest that the electronic structure of these materials is likely to be entirely different from that of the hole-doped ones, as verified by first-principles linearized muffin-tin orbital calculations.

Introduction

Rare-earth manganates of the formula $Ln_{1-x}A_xMnO_3$ (Ln = rare earth and A = alkaline earth) exhibit extraordinary properties such as colossal magnetoresistance (CMR) and charge ordering.[1] The manganates with $x < 0.5$, where the trivalent Ln ions are substituted by divalent A ions, have come to be designated as hole-doped. Accordingly, the manganates with $x > 0.5$, where the Ln ion substitutes a divalent A ion, are being referred to as electron-doped.[2] The manganates exhibiting CMR, by and large, have compositions in the range $0.1 < x < 0.5$, wherein the average radius of the A-site cations, $\langle r_A \rangle$, is fairly large. These manganates become ferromagnetic because of the double-exchange mechanism of electron hopping between Mn^{3+} ($t_{2g}^3e_g^1$) and Mn^{4+} ($t_{2g}^3e_g^0$) via the oxygen and undergo an insulator−metal transition around the ferromagnetic T_C. CMR is generally highest around T_C, and the T_C is sensitive to $\langle r_A \rangle$. When $\langle r_A \rangle$ is sufficiently small, the materials do not ordinarily exhibit ferromagnetism but instead become charge-ordered insulators. Thus, charge ordering and double exchange are competing interactions in the manganates. As x in $Ln_{1-x}A_xMnO_3$ increases, crossing over from the hole-doped regime to the electron-doped regime ($x > 0.5$), charge ordering becomes the dominant interaction and ferromagnetism does not appear to occur in any of the compositions. In this regime, CMR occurs over a narrow range of compositions, $0.80 < x < 1.0$, but there is no long-range ferromagnetism or metallicity associated with the materials.[2] The various features of the manganates are nicely borne out by the approximate phase diagrams shown in Figure 1, prepared on the basis of available data. What is noteworthy is the marked absence of symmetry in these phase diagrams. While the presence of electron−hole asymmetry in the manganates is not surprising, considering that the introduction of e_g electrons increases the lattice distortion and their removal would have the opposite effect, the asymmetry has some unusual features.

Electron−hole asymmetry is encountered in cuprate superconductors.[3] In the cuprates, superconductivity occurs in the electron-doped regime, although not as prominently as in the hole-doped regime. The electron−

* To whom correspondence should be addressed. E-mail: cnrrao@jncasr.ac.in.
[†] Jawaharlal Nehru Centre for Advanced Scientific Research.
[‡] Indian Institute of Science.
[§] University of California.

(1) (a) Ramirez, A. P. *J. Phys.*: *Condens. Matter* **1997**, *9*, 8171. (b) Rao, C. N. R., Raveau, B., Eds. *Colossal Magnetoresistance, Charge ordering and Related Properties of Manganese Oxides*; World Scientific: Singapore, 1998. (c) Rao, C. N. R.; Arulraj, A.; Cheetham, A. K.; Raveau, B. *J. Phys.*: *Condens. Matter* **2000**, *12*, R83.

(2) (a) Maignan, A.; Martin, C.; Damay, F.; Raveau, B. *Chem. Mater.* **1998**, *10*, 950. (b) Santhosh, P. N.; Arulraj, A.; Vanitha, P. V.; Singh, R. S.; Sooryanarayana, K.; Rao, C. N. R. *J. Phys.*: *Condens. Matter* **1999**, *11*, L27.

(3) Ramakrishnan, T. V.; Rao, C. N. R. *Superconductivity Today*, 2nd ed.; University of India Press: India, 1999.

10.1021/cm000464w CCC: $20.00
Published on Web 02/06/2001

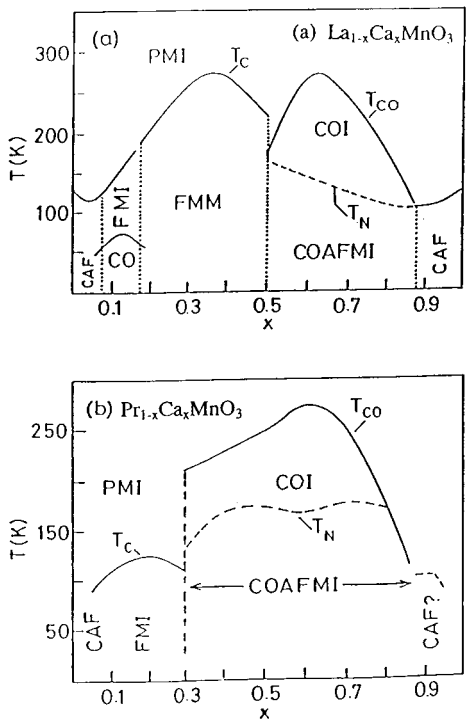

Figure 1. Phase diagrams of (a) $La_{1-x}Ca_xMnO_3$ and (b) $Pr_{1-x}Ca_xMnO_3$: CAF, canted antiferromagnet; CO, charge-ordered state; FMI, ferromagnetic insulator; FMM, ferromagnetic metal; PMI, paramagnetic insulator; COI, charge-ordered insulator (paramagnetic); COAFMI, charge-ordered antiferromagnetic insulator. These diagrams have been prepared based on the available data in the literature and reflect the properties of the systems fairly satisfactorily. The source material for diagram a can be found from ref 1c and from Cheong and Chen in ref 1b. The source material for diagram b can be found in ref 1b,c and in Maignan et al. *Phys. Rev. B* **1999**, *B60*, 12191.

hole asymmetry in the rare-earth manganates, involving the total absence of the ferromagnetic metallic (FMM) state in the electron-doped regime, is therefore worthy of investigation. We have studied this interesting problem by comparing the structural properties of the hole- and electron-doped manganates of similar compositions in the $Pr_{1-x}Ca_xMnO_3$ system ($x = 0.36$ and 0.64). Although there have been several studies on hole-doped compositions of this system,[1] a careful comparison of hole- and electron-doped materials seemed to be necessary. In particular, we have examined whether ferromagnetism can be induced in the electron-doped material by appropriate cation substitution in the B-site and/or application of magnetic fields. The cations chosen for this purpose are Cr^{3+} ($t_{2g}^3e_g^0$) and Ru^{4+} ($t_{2g}^4e_g^0$), which have been found to be effective in destroying charge ordering in materials such as $Nd_{0.5}Ca_{0.5}MnO_3$ and $Sm_{0.5}Ca_{0.5}MnO_3$.[4] To ensure that the Mn−O−Mn angle is not the limiting factor, we have prepared a manganate of the composition $La_{0.33}Ca_{0.33}Sr_{0.34}MnO_3$ with significantly large Mn−O−Mn angles and studied the effects of B-site substitution and magnetic fields on the properties of this material. We have also carried out first principles electronic structure calculations to understand what makes the hole- and electron-doped manganates different.

Experimental Section

Polycrystalline samples of the manganates were prepared by the ceramic method. Stoichiometric quantities of the respective rare-earth oxides, alkaline-earth carbonates, MnO_2 or Mn_3O_4, and the dopant transition-metal oxide (Cr_2O_3 or RuO_2) were mixed and preheated at 1173 K for 12 h in air. They were subsequently ground and heated at 1473 K for another 12 h in air. The mixture so obtained was pelletized and heated at 1673 K. The X-ray diffraction pattern recorded (using a Seifert XRD 3000TT instrument) showed a single phase for all of the compositions prepared. Rietveld analysis was carried using the structure refinement program GSAS. Data were collected between $2\theta = 10°$ and 100° with a scan step of 0.02°.

Electrical resistivity measurements were carried out on pressed pellets of polycrystalline materials by the four-probe method between 300 and 20 K. Magnetic measurements were carried out using a vibrating sample magnetometer (VSM-7300, Lakeshore Inc.) between 300 and 50 K employing a field of 0.01 T. Magnetoresistivity measurements were carried out using a cryocooled closed-cycle superconducting magnet designed by us along with Cryo Industries of America, Manchester, MA.

Results and Discussion

The phase diagrams of two rare-earth manganates, $Ln_{1-x}Ca_xMnO_3$ (Ln = La and Pr) in Figure 1, clearly demonstrate the electron−hole asymmetry present in these materials and also the preponderance of the charge-ordered (CO) state in the electron-doped regime ($x > 0.5$). The FMM state, generally found in the hole-doped regime ($x \leq 0.5$), is favored by the large size of the A-site cations.[5] Thus, the FMM state occurs up to $x = 0.5$ in $La_{1-x}Ca_xMnO_3$ (Figure 1a). In $Pr_{1-x}Ca_xMnO_3$, the FMM state is not found at any composition, and there is only a ferromagnetic insulating (FMI) state when $0.1 \leq x \leq 0.3$. The charge-ordering regime in $La_{1-x}Ca_xMnO_3$ is $0.5 \leq x \leq 0.85$ but is considerably wider ($0.3 \leq x \leq 0.85$) in $Pr_{1-x}Ca_xMnO_3$. Accordingly, charge ordering occurs in both the hole- and electron-doped compositions of the latter system. Charge ordering in these systems is ascertained by the appearance of superlattice reflections in the diffraction patterns and also by the occurrence of anomalies (observation of maxima) in the temperature variation of magnetic susceptibility and the activation energy for conduction.[1c]

Effects of Cation Size and Size Disorder. In Figure 2, we plot the charge-ordering transition temperatures, T_{CO}, in $Ln_{0.5}Ca_{0.5}MnO_3$ and $Ln_{0.36}Ca_{0.64}MnO_3$ against the average radius of the A-site cations $\langle r_A \rangle$. Here, $\langle r_A \rangle$ is varied by changing the Ln ion. While T_{CO} increases with a decrease in $\langle r_A \rangle$ in the case of $Ln_{0.5}Ca_{0.5}MnO_3$, it is not very sensitive to $\langle r_A \rangle$ in electron-doped $Ln_{0.36}Ca_{0.64}MnO_3$. In Table 1, we compare the T_{CO} values and other properties of $Ln_{0.64}Ca_{0.36}MnO_3$ and $Ln_{0.36}Ca_{0.64}MnO_3$. The T_{CO} value is generally higher in the latter system compared to that of the hole-doped materials, but there is little variation with $\langle r_A \rangle$ in both

(4) (a) Barnabe, A.; Maignan, A.; Hervieu, M.; Raveau, B. *Eur. Phys. J.* **1998**, *B1*, 145. (b) Barnabe, A.; Hervieu, M.; Martin, C.; Maignan, A.; Raveau, B. *J. Mater. Chem.* **1998**, *8*, 1405. (c) Martin, C.; Maignan, A.; Damay, F.; Hervieu, M.; Raveau, B. *J. Solid State Chem.* **1997**, *134*, 198. (d) Vanitha, P. V.; Arulraj, A.; Raju, A. R.; Rao, C. N. R. *C. R. Acad. Sci. Paris* **1999**, *2*, 595.

(5) (a) Hwang, H. Y.; Cheong, S. W.; Radaelli, P. G.; Marezio, M.; Batlogg, B. *Phys. Rev. Lett.* **1995**, *75*, 914. (b) Mahesh, R.; Mahendiran, R.; Raychaudhuri, A. K.; Rao, C. N. R. *J. Solid State Chem.* **1995**, *120*, 204.

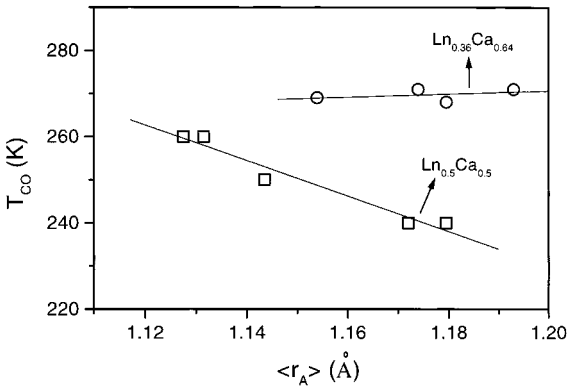

Figure 2. Variation of the charge-ordering transition temperature, T_{CO}, with the average size of the A-site cation, $\langle r_A \rangle$.

Table 1. Effect of $\langle r_A \rangle$ on Charge Ordering in $Ln_{1-x}Ca_xMnO_3$ ($x = 0.36$ and 0.64)

			lattice parameter (Å)			
Ln	$\langle r_A \rangle$ (Å)	σ^2 (Å^2)	*a*	*b*	*c*	T_{CO}[a] (K)
			$Ln_{0.64}Ca_{0.36}MnO_3$			
La	1.203	0.0003	5.454	5.468	7.704	*b*
Pr	1.179	0.0000	5.413	5.442	7.676	210
Nd	1.169	0.0001	5.407	5.458	7.646	212
			$Ln_{0.36}Ca_{0.64}MnO_3$			
La	1.193	0.0013	5.390	5.391	7.588	271
Pr	1.179	0.0000	5.374	5.369	7.576	268
Nd	1.174	0.0001	5.388	5.361	7.570	271

[a] From magnetization measurements ($H = 100$ G). [b] This compound exhibits ferromagnetism and an insultor−metal transition around the T_C (~250 K).

series of compounds. In the series of manganates listed in Table 1, the cation size disorder,[6a] as measured by the variance, σ^2, is quite small. It may be noted that in the electron-doped manganates T_{CO} increases with electron concentration, *x*, but the ferromagnetic component[2a] (in the cluster regime $0.0 < x < 0.2$ in $Ca_{1-x}Ln_xMnO_3$) is only slightly affected by $\langle r_A \rangle$ for a fixed value of *x*.

The effect of cation size disorder on the charge-ordering transition in $Ln_{0.5}Ca_{0.5}MnO_3$ has been investigated by keeping the average radius of the A-site cation fixed and varying σ^2. The value of σ^2 is varied by making different combinations of the Ln and alkaline-earth ions.[6b] The slope of the linear $T_{CO}-\sigma^2$ plot for $Ln_{0.5}Ca_{0.5}MnO_3$ is 10 975 K Å^{-2} and the intercept of the plot, T_{CO}^0, is 236 K. The value of T_{CO}^0 corresponds to that of the disorder-free manganate. We have not been able to obtain sufficient reliable data on the variation of T_{CO} with σ^2 (at fixed $\langle r_A \rangle$) in hole-doped compositions of the type $Ln_{0.64}Ca_{0.36}MnO_3$, but the limited data available show only small changes. In the case of the electron-doped $Ln_{0.36}Ca_{0.64}MnO_3$, however, we have obtained reliable data for two series of manganates with fixed $\langle r_A \rangle$ values of 1.180 and 1.174 Å, respectively, corresponding to $Pr_{0.36}Ca_{0.64}MnO_3$ and $Nd_{0.36}Ca_{0.64}MnO_3$. These compounds, along with their structural data and T_{CO} values, are listed in Table 2. We show the plots of T_{CO} against σ^2 for the two series of manganates in Figure 3. The plots are linear, giving slopes 6408 and 5813 K Å^{-2} for fixed $\langle r_A \rangle$ of 1.180 and 1.174 Å, respectively. The intercept, T_{CO}^0, is around 266 K in both of the cases, a value considerably higher than that in $Ln_{0.5}A_{0.5}MnO_3$.[6b] An examination of the phase diagram in Figure 1a shows that in $La_{1-x}Ca_xMnO_3$ T_{CO} reaches a maximum value around $x = 0.65$. We see a similar maximum in the phase diagram of $Pr_{1-x}Ca_xMnO_3$ as well (Figure 1b). In the latter system, however, T_{CO} increases with the hole concentration, *x*, in the hole-doped regime ($0.3 < x \leq 0.5$) and with the electron concentration, $1 - x$, in the electron-doped regime ($0.6 < x \leq 0.85$). Despite some of these apparent similarities, the hole-doped and electron-doped compositions exhibit significant differences in their electronic and magnetic properties, as detailed in the following sections.

Comparison of the Hole- and Electron-Doped $Pr_{1-x}Ca_xMnO_3$ ($x = 0.36$ and 0.64). To understand the nature of electron−hole asymmetry in the rare-earth manganates, it is useful to compare the electronic and magnetic properties of comparable compositions of the hole- and electron-doped materials. Thus, the hole-doped $La_{0.7}Ca_{0.3}MnO_3$ becomes ferromagnetic around 250 K, at which temperature it exhibits an insulator−metal transition. The electron-doped $La_{0.3}Ca_{0.7}MnO_3$, on the other hand, gets charge-ordered at 271 K and does not exhibit the FMM state at any temperature. A better appreciation of the differences in the properties of the hole- and electron-doped manganates is obtained by comparing the properties of $Pr_{1-x}Ca_xMnO_3$ at the same carrier concentration (equal values of $1 - x$ and *x*). We have carried out detailed studies on $Pr_{0.64}Ca_{0.36}MnO_3$ and $Pr_{0.36}Ca_{0.64}MnO_3$, both of which are charge-ordered.

$Pr_{0.64}Ca_{0.36}MnO_3$, I, and $Pr_{0.36}Ca_{0.64}MnO_3$, II, are both orthorhombic (*Pbnm*), but the unit cell is larger in the former as expected on the basis of the relative sizes of Mn^{3+} and Mn^{4+}. In Table 3, we list the atomic coordinates and the lattice parameters of the two manganates obtained from the Rietveld analysis. The Mn−O distances in I are longer than those in II, but the Mn−O−Mn angles in the two are comparable.

Both $Pr_{0.64}Ca_{0.36}MnO_3$ and $Pr_{0.36}Ca_{0.64}MnO_3$ get charge-ordered in the paramagnetic state, with transition temperatures (T_{CO}) of 210 and 268 K, respectively. They show maxima in the magnetization curves at the charge-ordering transition temperatures (Figure 4). $Pr_{0.64}Ca_{0.36}MnO_3$ also shows an antiferromagnetic transition around 140 K. The nature of the transitions has been ascertained independently by diffraction studies as well as EPR and other measurements.[1,7] Both $Pr_{0.64}Ca_{0.36}MnO_3$ and $Pr_{0.36}Ca_{0.64}MnO_3$ are insulators down to low temperatures, as is expected of charge-ordered compositions, but the electron-doped composition shows a more marked change in resistivity at T_{CO} (Figure 5). The difference between the two lies in the effect of magnetic fields. Application of a magnetic field of 12 T melts the CO state to a metallic state in the case of $Pr_{0.64}Ca_{0.36}MnO_3$ (Figure 5a). A 12 T magnetic field has no effect whatsoever on the resistivity of $Pr_{0.36}Ca_{0.64}MnO_3$ (Figure 5b).

Substitution of Cr^{3+} or Ru^{4+} in the Mn site of certain charge-ordered manganates is known to destroy the CO state, rendering them ferromagnetic and metallic.[1c,4,8] The effect of Cr^{3+} doping on $Pr_{1-x}Ca_xMnO_3$ has been

(6) (a) Rodriguez-Martinez, L. M.; Attfield, J. P. *Phys. Rev.* **1996**, *B54*, R15622; **1998**, *B58*, 2426. (b) Vanitha, P. V.; Santhosh, P. N.; Singh, R. S.; Rao, C. N. R.; Attfield, J. P. *Phys. Rev.* **1999**, *B59*, 13539.

(7) Gupta, R.; Joshi, J. P.; Bhat, S. V.; Sood, A. K.; Rao, C. N. R. *J. Phys.: Condens. Matter* **2000**, *12*, 6919.

Table 2. Structure and Properties of $Ln_{0.36-x}LnCa_xCa_{0.64-y}Sr_yMnO_3$ with Fixed $\langle r_A \rangle$ Values[a]

composition	σ^2 (Å^2)	lattice parameter (Å)			% D (300 K)	T_{CO} (K)
		a	*b*	*c*		
		$\langle r_A \rangle = 1.174$ Å				
$Nd_{0.36}Ca_{0.64}MnO_3$	0.0001	5.388	5.361	7.570	0.33	271 (261)
$Pr_{0.28}Gd_{0.08}Ca_{0.64}MnO_3$	0.0003	5.353	5.366	7.548	0.18	279 (270)
$La_{0.185}Gd_{0.175}Ca_{0.64}MnO_3$	0.0011	5.354	5.369	7.537	0.27	257 (253)
$La_{0.225}Y_{0.135}Ca_{0.64}MnO_3$	0.0017	5.353	5.370	7.563	0.15	249 (248)
$Sm_{0.36}Ca_{0.554}Sr_{0.086}MnO_3$	0.0022	5.355	5.372	7.569	0.15	263 (258)
$Nd_{0.1}Gd_{0.26}Ca_{0.528}Sr_{0.112}MnO_3$	0.0033	5.355	5.364	7.580	0.06	245 (243)
$Gd_{0.15}Y_{0.21}Ca_{0.433}Sr_{0.207}MnO_3$	0.0066	5.346	5.374	7.567	0.21	~229 (223)
		$\langle r_A \rangle = 1.18$ Å				
$Pr_{0.36}Ca_{0.64}MnO_3$	0.0000	5.374	5.369	7.576	0.11	267 (267)
$Nd_{0.18}Sm_{0.18}Ca_{0.553}Sr_{0.087}MnO_3$	0.0019	5.369	5.370	7.580	0.07	~256 (251)
$Nd_{0.18}Gd_{0.18}Ca_{0.518}Sr_{0.122}MnO_3$	0.0031	5.363	5.376	7.573	0.14	250 (245)
$La_{0.16}Y_{0.2}Ca_{0.526}Sr_{0.114}MnO_3$	0.0043	5.364	5.370	7.578	0.07	~241 (~238)
$La_{0.1}Y_{0.26}Ca_{0.46}Sr_{0.18}MnO_3$	0.0060	5.386	5.369	7.550	0.32	234 (222)

[a] The values in parentheses are obtained from resistivity data; % D is the orthorhombic distortion.

Table 3. Atomic Coordinates and Structural Parameters of I, $Pr_{0.64}Ca_{0.36}MnO_3$,[a] and II, $Pr_{0.36}Ca_{0.64}MnO_3$[b]

atom	site	*x*	*y*	*z*	frac	U_{ISO}
Pr	4c	−0.0083 (0.5027)	0.0315 (0.4746)	0.2500 (0.2500)	0.6400 (0.3600)	0.0049 (−0.0033)
Ca	4c	−0.0083 (0.5027)	0.0315 (0.4746)	0.2500 (0.2500)	0.3600 (0.6400)	0.0049 (−0.0033)
Mn	4b	0.5000 (0.5000)	0.0000 (0.0000)	0.0000 (0.0000)	1.0000 (1.0000)	0.0040 (0.0063)
O	8d	0.0529 (0.0544)	0.4939 (0.5213)	0.2500 (0.2500)	1.0000 (1.0000)	0.0405 (0.0901)
O	4c	−0.7115 (0.2854)	0.2809 (0.2717)	0.0354 (−0.0460)	1.0000 (1.0000)	0.0122 (−0.0367)

bond	distance (Å)	bond	angle (deg)
Mn−O	2 × 1.935 (2 × 1.892)	Mn−O−Mn	4 × 157.6 (4 × 155.6)
	2 × 1.941 (2 × 1.993)		2 × 162.9 (2 × 161.2)
	2 × 1.989 (2 × 1.916)		

[a] $a = 5.4310$ Å, $b = 5.4573$ Å, $c = 7.6761$ Å; *Pbnm*; $R_{wp} = 3.45\%$. [b] $a = 5.3664$ Å, $b = 5.3746$ Å, $c = 7.5603$ Å; *Pbnm*; $R_{wp} = 3.28\%$. The values in brackets correspond to those of II.

investigated in the composition region $0.6 \leq x \leq 0.7$, with the Cr^{3+} content going up to 12%.[4a] These workers find a marked effect when Cr^{3+} is around 10%, at which composition one would expect clustering of the dopant ions leading to superexchange-induced ferromagnetism. We have substituted Mn by Cr^{3+} or Ru^{4+}, keeping the dopant concentration at 3% to avoid clustering. On doping with 3% Cr^{3+}, $Pr_{0.64}Ca_{0.36}MnO_3$ becomes ferromagnetic with a T_C of 130 K, but $Pr_{0.36}Ca_{0.64}MnO_3$ remains paramagnetic and charge-ordered, albeit with a slightly lower T_{CO} (215 K) as shown in Figure 6a. The 3% Ru doping shows similar differences between the two manganates (Figure 6b).

In Figure 7, we show the effect of 3% Cr^{3+} doping on the resistivity of $Pr_{0.64}Ca_{0.36}MnO_3$ and $Pr_{0.36}Ca_{0.64}MnO_3$. The former exhibits an insulator−metal (I−M) type transition around 80 K, but the latter remains an insulator. The I−M transition in the hole-doped system is shifted to higher temperatures on applying magnetic fields. Application of magnetic fields does not render the Cr^{3+}-doped $Pr_{0.36}Ca_{0.64}MnO_3$ metallic (Figure 7) at any temperature, indicating that it may not be possible to induce the FMM state in this electron-doped material even under favorable conditions. Results with 3% Ru^{4+} doping in the two manganates are similar, in that the hole-doped material becomes FMM while the CO state in the electron-doped material is essentially unaffected. In the insets of Figure 7, we show the results obtained with 3% Ru^{4+}-doped $Pr_{0.64}Ca_{0.36}MnO_3$ and $Pr_{0.36}Ca_{0.64}MnO_3$. The failure to destroy the CO state of $Pr_{0.36}Ca_{0.64}MnO_3$ with Cr/Ru doping as well as with a magnetic

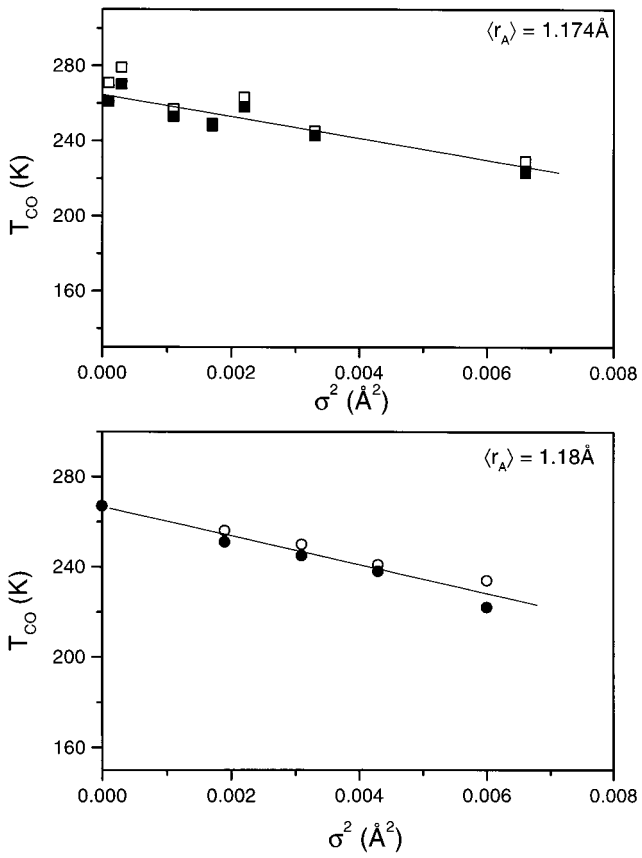

Figure 3. Variation of the charge-ordering temperature in $Ln_{0.36}Ca_{0.64}MnO_3$ with σ^2 for fixed $\langle r_A \rangle$ values. Open symbols represent data obtained from magnetic measurements, and the corresponding closed symbols are from resistivity measurements.

(8) (a) Raveau, B.; Maignan, A.; Martin, C.; Hervieu, M. *Chem. Mater.* **1998**, *10*, 2641. (b) Vanitha, P. V.; Singh, R. S.; Natarajan, S.; Rao, C. N. R. *J. Solid State Chem.* **1998**, *137*, 365.

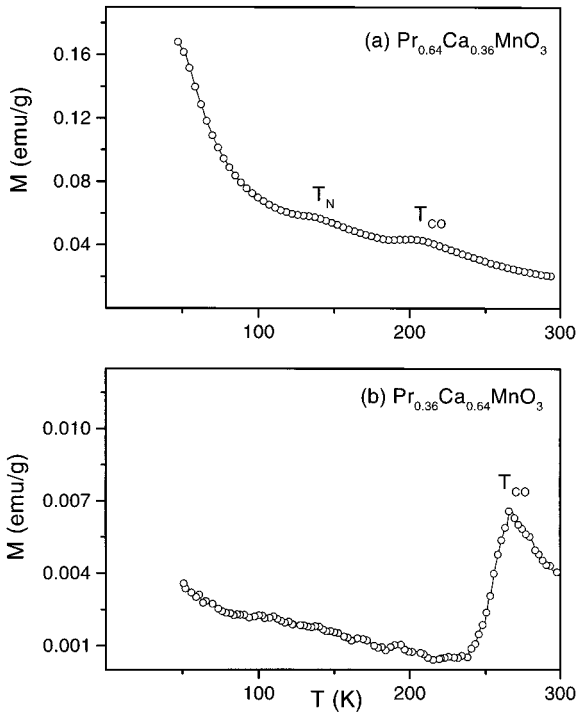

Figure 4. Temperature variation of the magnetization of (a) $Pr_{0.64}Ca_{0.36}MnO_3$ and (b) $Pr_{0.36}Ca_{0.64}MnO_3$.

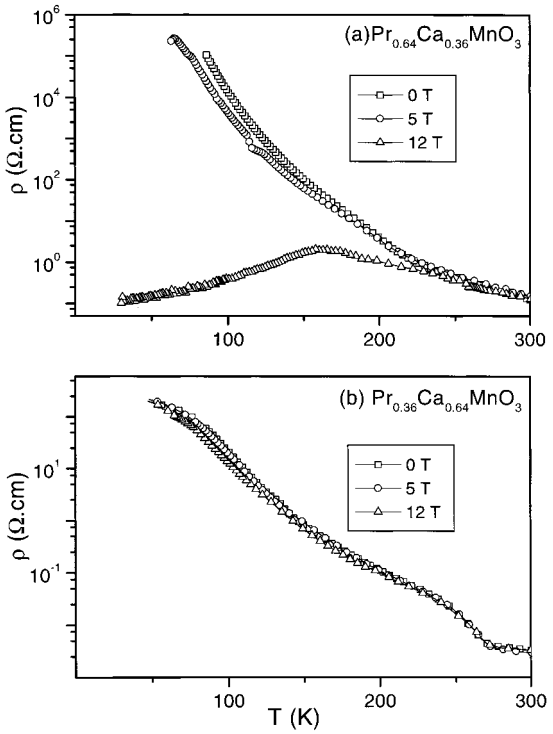

Figure 5. Temperature variation of the electrical reisistivity of (a) $Pr_{0.64}Ca_{0.36}MnO_3$ and (b) $Pr_{0.36}Ca_{0.64}MnO_3$. The effect of magnetic fields is shown.

field of 12 T is noteworthy. Raveau et al.[9] have recently observed that Ru substitution in $Ln_{0.4}Ca_{0.6}MnO_3$ gives rise to FMM clusters, but the effect is prominent at high Ru concentrations (>3%). The observed effect is probably due to clusters or domains containing Ru ions, as suspected by these authors. Furthermore, the observed

(9) Raveau, B.; Maignan, A.; Martin, C.; Mahendiran, R.; Hervieu, M. *J. Solid State Chem.* **2000**, *151*, 330.

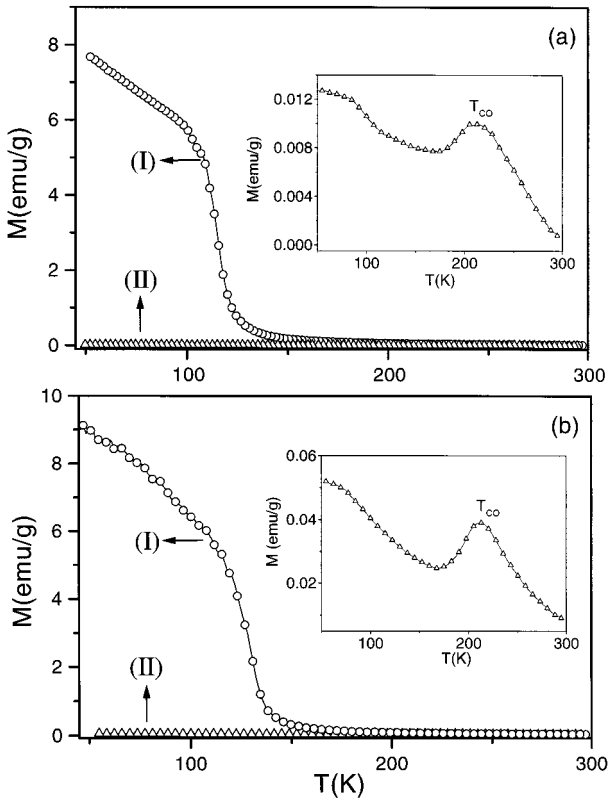

Figure 6. Effect of (a) 3% Cr doping and (b) 3% Ru doping in the Mn site of $Pr_{0.64}Ca_{0.36}MnO_3$, I, and $Pr_{0.36}Ca_{0.64}MnO_3$, II, on the magnetization. The inset gives the magnetization data of II on an enlarged scale to show T_{CO}.

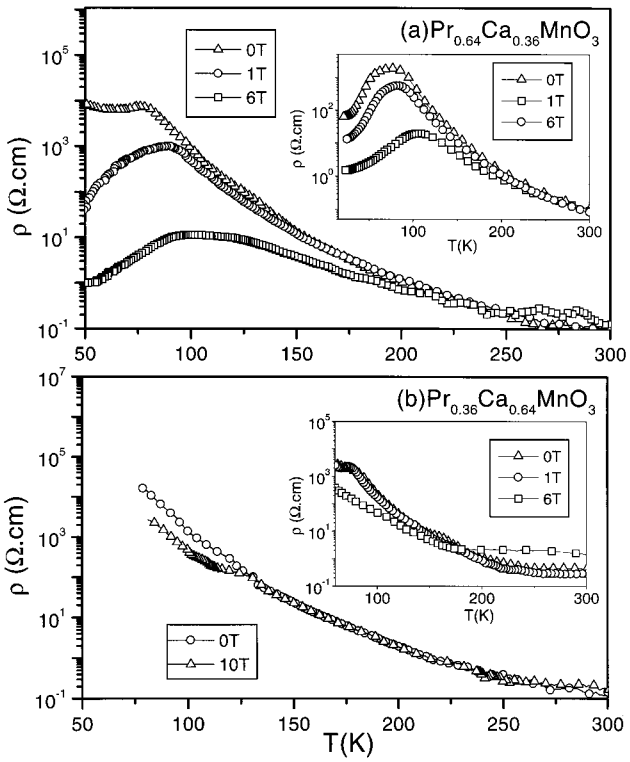

Figure 7. Effect of 3% Cr^{3+} doping on the electrical resistivity of (a) $Pr_{0.64}Ca_{0.36}MnO_3$ and (b) $Pr_{0.36}Ca_{0.64}MnO_3$. The effect of magnetic fields is also shown. Insets in a and b show the effect of 3% Ru doping.

magnetization in these samples is low. This raises the question as to whether long-range ferromagnetism can ever occur in the electron-doped manganates. We note

Table 4. Atomic Coordinates and Structural Parameters of $La_{0.33}Ca_{0.33}Sr_{0.34}MnO_3$[a]

atom	site	*x*	*y*	*z*	frac	U_{ISO}
La	4b	0.0000	0.5000	0.2500	0.3300	−0.0134
Ca	4b	0.0000	0.5000	0.2500	0.3300	0.0245
Sr	4b	0.0000	0.5000	0.2500	0.3400	0.0212
Mn	4c	0.0000	0.0000	0.0000	1.0000	0.0007
O	4a	0.0000	0.0000	0.2500	1.0000	0.0051
O	8h	0.2799	0.7799	0.0000	1.0000	0.0051

bond	distance (Å)	bond	angle (deg)
Mn−O	4 × 1.909	Mn−O−Mn	4 × 166.4
	2 × 1.949		2 × 180.0

[a] $a = b = 5.3608$ Å, $c = 7.7857$ Å; *I*4/*mcm*; $R_{wp} = 11.82\%$.

here that Maignan et al.[10] find a cluster glass state (but no long-range ferromagnetism) in $Ca_{1-x}Sm_xMnO_3$ ($0 \leq x \leq 0.12$). Neumeier and Cohn[11] observe only local ferromagnetic regions within an antiferromagnetic host in $Ca_{1-x}La_xMnO_3$ ($0 \leq x \leq 0.2$), as was indeed observed earlier by Mahendiran et al.[12]

Absence of Long-Range Ferromagnetism in Electron-Doped Manganates. To answer the above question, it is important to ensure that the Mn−O−Mn angle is not a limiting factor. This is because the Mn−O−Mn angle in $Pr_{1-x}Ca_xMnO_3$ is generally in the 156−162° range (Table 3), which may be considered to be somewhat small. For ferromagnetism to be favored in the electron-doped manganates, it is important to have a material with a much larger Mn−O−Mn angle. To decide on the composition of such a material, the following considerations are relevant. The Mn−O−Mn angles in $CaMnO_3$ and $La_{0.5}Ca_{0.5}MnO_3$ are around 158° and 160°, respectively.[13,14] Therefore, substitution of Ca by any of the rare earths would not increase the Mn−O−Mn angle beyond 160°. It is, however, possible to increase the angle by Sr substitution, as in $Ca_{1-x}Sr_xMnO_3$ and $La_{0.5}Ca_{0.5-x}Sr_xMnO_3$.[15,16] We therefore prepared a manganate of the composition $La_{0.33}Ca_{0.33}Sr_{0.34}MnO_3$. The structure of the manganate is tetragonal (*I*4/*mcm*). On the basis of a Rietveld analysis of the powder X-ray diffraction data, we have obtained the atomic coordinates and structural parameters listed in Table 4. The two Mn−O−Mn distances are around 1.91 and 1.95 Å, while the angles are 166.4° and 180°. These values of the angles are comparable to those found in some of the ferromagnetic and metallic compositions of the hole-doped manganates.

In Figure 8 we show the magnetization and electrical resistivity data of $La_{0.33}Ca_{0.33}Sr_{0.34}MnO_3$. The material is a paramagnetic insulator down to 25 K, with a charge-ordering transition of around 220 K. Application of magnetic fields up to 12 T has no effect on the electrical

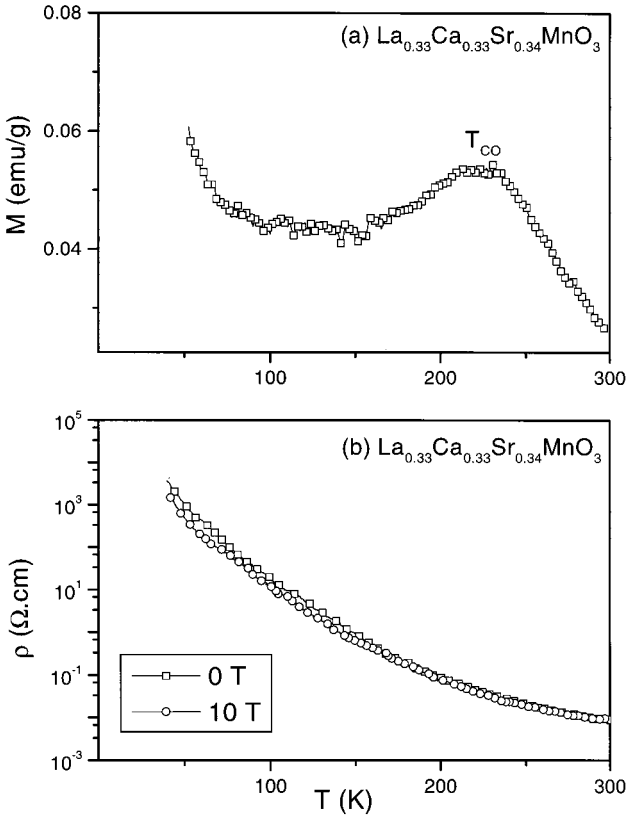

Figure 8. Temperature variation of (a) the magnetization and (b) the resistivity of $La_{0.33}Ca_{0.33}Sr_{0.34}MnO_3$. The effect of magnetic fields on the resistivity is shown.

resistivity (Figure 8b). Clearly, the large Mn−O−Mn angles do not help to make this manganate ferromagnetic. Furthermore, 3% Cr^{3+} doping of $La_{0.33}Ca_{0.33}Sr_{0.34}MnO_3$ does not transform it to a ferromagnetic metal (Figure 9). What is surprising is that the application of magnetic fields up to 10 T does not induce an I−M transition in the Cr-doped material. The same holds for the 3% Ru^{4+}-doped material, as shown in the insets of Figure 9a,b. It must be remembered that the analogous hole-doped composition $La_{0.67}A_{0.33}MnO_3$ (A = Ca/Sr) becomes a ferromagnetic metal at fairly high temperatures (230−300 K).[1] These results suggest that it may not be possible to make the electron-doped rare-earth manganates exhibit long-range ferromagnetism and metallicity. As observed earlier, other studies also show at best local ferromagnetic interactions or the presence of FM clusters.[9−12]

The absence of long-range ferromagnetism and metallicity in the electron-doped manganates is difficult to comprehend. One difference that is noteworthy is that the hole-doped manganates possess a higher proportion of e_g electrons relative to the degenerate e_g orbitals. There are also some intrinsic differences between the Mn^{3+} (d^4) and Mn^{4+} (d^3) ions. Although the structure of the parent $LnMnO_3$ compounds is influenced by the Jahn−Teller distorted Mn^{3+}, the stability of this state is not sufficient to inhibit the electron-transfer process when Mn^{4+} ions are introduced. The facile electron transfer required for double exchange, and hence ferromagnetism, can be sustained in such a hole-doped system. By contrast, the high ligand-field stabilization of the preponderant Mn^{4+} ions in the electron-doped materials can inhibit electron transfer. To unravel the

(10) Maignan, A.; Martin, C.; Damay, F.; Raveau, B.; Hejtmanek, J. *Phys. Rev.* **1998**, *B58*, 2758.
(11) Neumeier, J. J.; Cohn, J. L. *Phys. Rev.* **2000**, *B61*, 14319.
(12) Mahendiran, R.; Tiwary, S. K.; Raychaudhuri, A. K.; Ramakrishnan, T. V.; Mahesh, R.; Rangavittal, N.; Rao, C. N. R. *Phys. Rev.* **1996**, *B53*, 3348.
(13) Poeppelmeirer, K. R.; Leonowicz, M. E.; Scanlon, J. C.; Longo, J. M.; Yellon, W. B. *J. Solid State Chem.* **1982**, *45*, 71.
(14) Radaelli, P. G.; Cox, D. E.; Marezio, M.; Cheong, S. W.; Schiffer, P. E.; Ramirez, A. P. *Phys. Rev. Lett.* **1995**, *75*, 4488. (b) Radaelli, P. G.; Cox, D. E.; Capogna, L.; Cheong, S.-W.; Marezio, M. *Phys. Rev.* **1999**, *B59*, 14440.
(15) Taguchi, H.; Sonoda, M.; Nagao, M. *J. Solid State Chem.* **1998**, *137*, 82.
(16) Sundaresan, A.; Paulose, P. L.; Mallik, R.; Sampathkumaran, E. V. *Phys. Rev.* **1998**, *B57*, 2690.

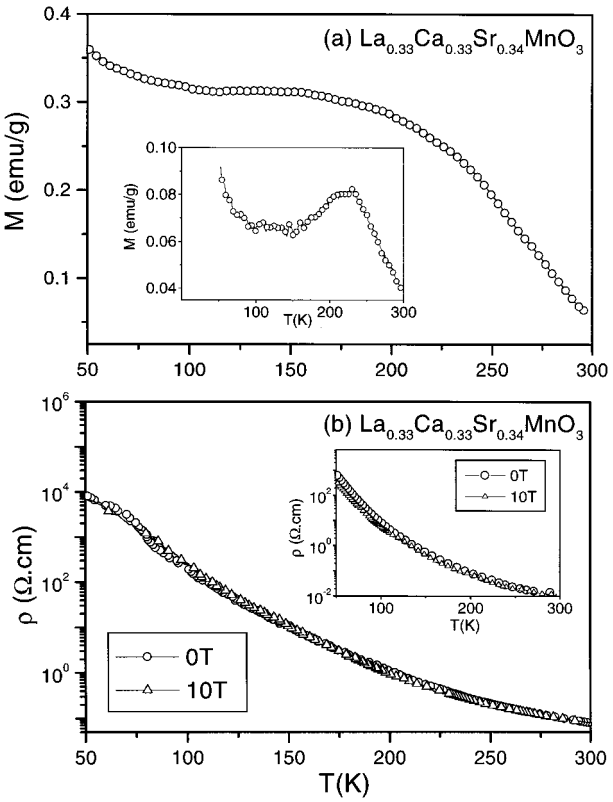

Figure 9. Effect of 3% Cr^{3+} doping on (a) the magnetization and (b) the resistivity of $La_{0.33}Ca_{0.33}Sr_{0.34}MnO_3$. The effect of magnetic fields on the resistivity is also shown. Insets in a and b show the effect of 3% Ru doping.

cause(s) for the absence of metallicity in the electron-doped managanates, we have carried out some electronic structure calculations.

Electronic Structure Calculations. We have used first-principles electronic structure calculations as manifest in the (spin) density functional linearized muffin-tin orbital method to examine whether the asymmetry in properties is reflected in a corresponding asymmetry in the one-electron band structure. While in a more complete analysis explicit electron correlation of the Hubbard U type would be intrinsic to the calculation,[17] we have taken the view that one-electron bandwidths point to the possible role that correlation might play and that correlation could be a consequence of the one-electron band structure rather than an integral part of the electronic structure. We have chosen the $La_{1-x}Ca_xMnO_3$ system for our calculations to avoid complications due to 4f electrons in the corresponding Pr system.

For our calculations on $La_3CaMn_4O_{12}$ ($La_{0.75}Ca_{0.25}MnO_3$), we have used the structure reported by Radaelli et al.[14] refined from powder neutron diffraction data on 20 K. Ordering La and Ca in a supercell yields a structure with the same lattice parameters but in the space group *Pm* with 14 atoms (rather than 4) in the asymmetric unit. This structure is displayed in Figure 10. La and Ca have closely similar radii, and ordering them over crystallographically distinct sites is unphysical. However, the bond lengths and angles in the structures used in our calculations closely follow the experiments. For the electron-doped $La_{0.25}Ca_{0.75}MnO_3$

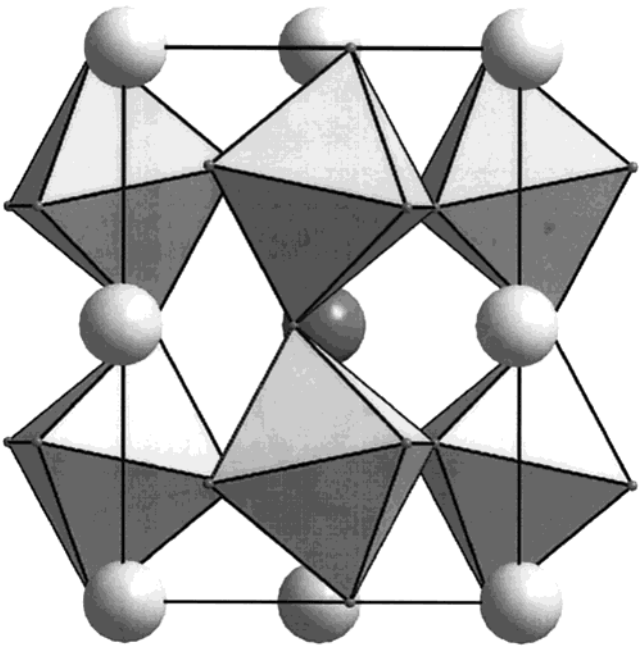

Figure 10. Monoclinic (space group *Pm*) structure of $La_3CaMn_4O_{12}$. The dark spheres are La, and the light sphere is Ca. The view is looking down the short $a = a_P\sqrt{2}$ axis.

($LaCa_3Mn_4O_{12}$), we have used the cell and positional parameters of the refined 300 K neutron powder diffraction structure of $La_{0.33}Ca_{0.67}MnO_3$ from Radaelli et al.[14] Again, the supercell is in the space group *Pm* rather than in the orthorhombic *Pnma* space group. Calculations were performed using the Stuttgart TB-LMTO-ASA program.[18] The basis sets consisted of 6s, 5d, and 4f orbitals for La, 4s and 3d orbitals for Ca, 4s, 4p, and 3d orbitals for Mn, and 2p orbitals for O. The atomic sphere approximation (ASA) relies on the partitioning of space into atom-centered spheres as well as empty spheres, with the latter being critical in structures that are not closely packed. The basis for the empty spheres is 1s orbitals, with the 2p component treated using downfolding. The spheres are chosen so that the atom-centered spheres do not have a volume overlap of more than 16%. The calculations used 108K points in the primitive Brillouin zone for achieving convergence. Because of the *Pm* supercell employed, the nature of the magnetism becomes a little more complex and perhaps artificial for both of the systems studied. Indeed, there are now two types of somewhat indistinct Mn atoms in the unit cell. We have found a tendency for a ferrimagnetic ground state in both of the manganates, with the two Mn having opposite spins. For simplifying the comparison of the two electronic structures, the Mn atoms were provided similar polarization at the start of the calculations; self-consistency yielded a ferromagnet in both of the cases.

The calculations yielded a ferromagnetic ground state with a magnetic moment of 3.2 μ_B per Mn for $La_3CaMn_4O_{12}$ (spin-only value 3.75 μ_B). Such a reduction in the magnetic moment from the expected value can arise because of an infelicitous choice of sphere radii and does not merit interpretation. The refined neutron moment

(17) Anisimov, V. I.; Zaanen, J.; Andersen, O. K. *Phys. Rev.* **1991**, *B48*, 943.

(18) Andersen, O. K.; Jepsen, O.; et al. *The Stuttgart TB-LMTO-ASA-47 Program*; MPI für Feukörperforschung: Stuttgart, 1998. (b) Skriver, H. L. *The LMTO Method*; Springer: Berlin, 1984.

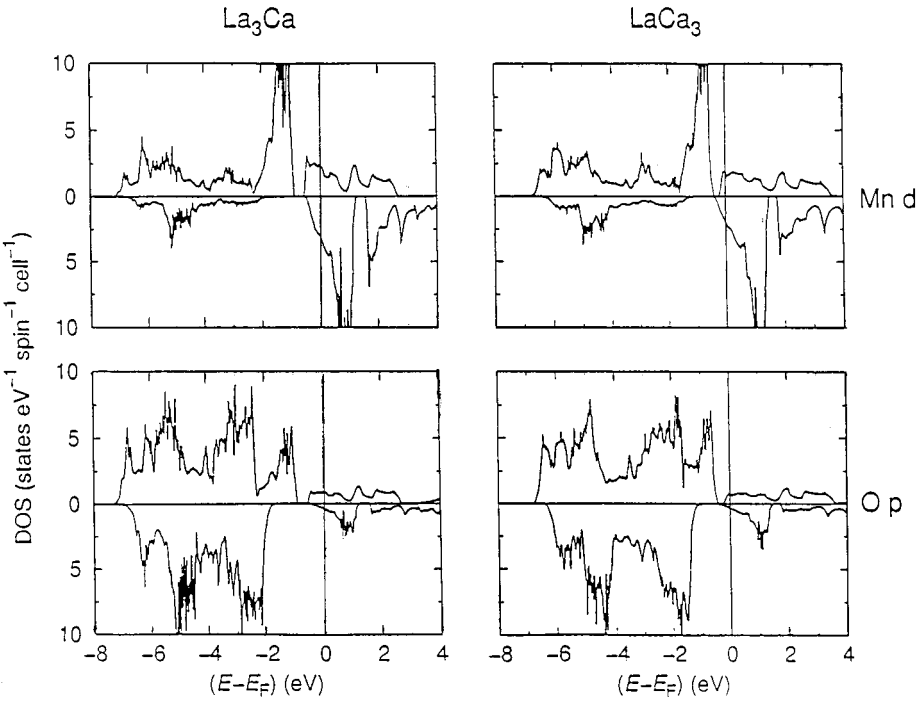

Figure 11. LMTO DOS for Mn and O in $La_3CaMn_4O_{12}$ and $LaCa_3Mn_4O_{12}$ near the Fermi energy. The upper halves of each panel display up-spin states, and the lower halves, down-spin states.

on Mn is 3.5 μ_B.[14] For ferromagnetic $LaCa_3Mn_4O_{12}$, the calculated magnetic moment was 3 μ_B (spin-only value 3.25). Figure 11 compares the spin-polarized densities of state (DOS) in the two spin directions for Mn and O in the two compositions. In each panel, the majority up-spin states are depicted in the upper half and the minority down-spin states in the lower half.

In both of the manganates, we find filled localized t_{2g}^3 (↑) states with a small bandwidth, of the order of 1.5 eV, polarizing a broader conduction band that is essentially e_g (↑) derived, although some t_{2g} (↓) states also occur at the Fermi energy. In $La_3CaMn_4O_{12}$, the Fermi energy E_F lies in a relatively broad conduction band. Both Mn and O states are present at E_F, indicating some covalency. Of note is the spin differentiation at the Fermi energy, with there being significantly more down-spin Mn states at the E_F than up-spin states. In the case of $LaCa_3Mn_4O_{12}$, E_F again lies in an e_g (↑) derived conduction band, but because of the smaller number of e_g electrons, E_F is at the band edge. Through examination of the so-called "fat-bands" (energy bands that have been decorated with the character of the corresponding orthonormal orbitals), we know that the e_g states in the perovskite systems[19] are derived from the combination of the narrow d_z^2 bands and the broader bands formed by the strong covalent overlap between O p_x and p_y and metal $d_{x^2-y^2}$ orbitals. A scheme depicting the nature of the overlap is displayed in Figure 12. In $LaCa_3Mn_4O_{12}$, where there is a much smaller filling of the e_g, it is the relatively narrow d_{z^2}-derived band that is mostly occupied. The finding that E_F lies on a band edge suggests that this oxide would be susceptible to the opening of a gap in the DOS at E_F, through correlations of the Hubbard type. At the same time, the propensity for the localized and delocalized states to be separated through a mobility edge (the formation of an Anderson insulator)

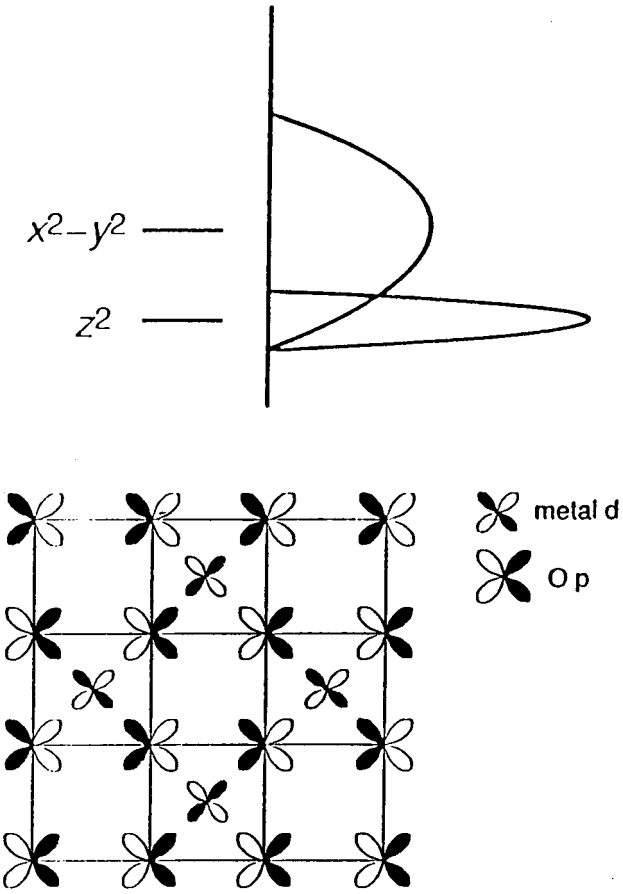

Figure 12. Scheme displaying the Jahn−Teller distorted e_g states becoming bands in solids such as perovskite manganese oxides. Because of overlap between metal $d_{x^2-y^2}$ and O p_x and p_y, the $d_{x^2-y^2}$-derived bands are significantly broader. A scheme for such overlap is displayed along the *ab* plane.

(19) Felser, C.; Seshadri, R.; Leist, A.; Tremel, W. *J. Mater. Chem.* **1998**, *8*, 787.

is also increased by E_F lying on a band edge. In systems such as the present ones, disorder due to disparate ions occupying the A site of the perovskite structure cannot be avoided. A point of interest is that in $LaCa_3Mn_4O_{12}$ the DOS at E_F shows a smaller spin differentiation than that in $La_3CaMn_4O_{12}$. Spin differentiation is believed to be the key to the unusual magnetic field dependence of the electrical transport properties such as colossal magnetoresistance.[20] This suggests that the electron-doped manganates may be less interesting with respect to the CMR properties.

Conclusions

The electron-doped regime ($x > 0.5$) of the rare_earth manganates of the general formula $Ln_{1-x}Ca_xMnO_3$ is dominated by charge-ordering effects. While the effects of cation size and size disorder on the charge-ordered states of the hole- and electron-doped compositions are similar, their properties vary markedly as revealed by the comparison of the properties of the hole-doped $Pr_{0.64}Ca_{0.36}MnO_3$ and the electron-doped $Pr_{0.36}Ca_{0.64}MnO_3$. The CO state of the former is transformed to the FMM state by magnetic fields as well as by 3% Cr^{3+} or Ru^{4+} substitution in the Mn site, but none of these affects the CO state of the electron-doped material, which remains a paramagnetic insulator under all conditions. Increasing the Mn−O−Mn angle from 158 to 162°, as in the above two manganates, to 165−180° in $La_{0.33}Ca_{0.33}Sr_{0.34}MnO_3$ does not result in ferromagnetism and metallicity. The CO state in this material is also unaffected by magnetic fields and Cr^{3+}/Ru^{4+} substitution in the Mn site. We are, therefore, prompted to conclude that it is not possible to induce long-range ferromagnetism in the electron-doped manganates by any means. First-principles calculations suggest that this may be because the Fermi level lies on a band edge in these materials.

Acknowledgment. This work was partially supported by the MRSEC Program of the NSF under Grant DMR 96-32716.

CM000464W

(20) Pickett, W. E.; Singh, D. J. *Phys. Rev.* **1996**, *B53*, 1146.